PREPARATION AND CHARACTERIZATION OF CHITOSAN -LIGNIN BIOCOMPOSITE MATERIALS DERIVED FROM WASTE OF *TERMINALIA CATAPPA* LEAVE AS DOXORUBICIN LOADED ANTICANCER DRUG CARRIER AGENT*

Aung Than Htwe[1], May Thazin Kyaw[2]

Abstract

Doxorubicin (DOX) is known to be an effective treatment for various cancer types, including breast and ovarian cancer. In this paper, chitosan-lignin biocomposite particles are prepared by combining chitosan and lignin. Lignin is extracted from the waste of *Terminalia catappa* leaves. The obtained chitosan-lignin (CSLN) biocomposite particles were used as a potential candidate for controlled release of the anticancer drug doxorubicin (DOX). The CSLN biocomposite was characterized using FT-IR, XRD, SEM, TGDTA, and UV-vis. The FTIR data confirmed the formation of chemical bonds between the components of the obtained composites. The SEM data demonstrated that the lignin introduction had caused significant changes in the surface morphology of biocomposite. These biocomposite materials have been studied as a function of lignin, indicating that the thermal stability of the chitosan gel is enhanced. Furthermore, the samples were assessed for gel content, swelling properties, and drug release. The swelling and drug release profiles revealed that the amount of drug released and swelling of the composite depended on the CS content, LN content, and pH of biocomposite content. Prolonged and more controlled drug releases were observed for CSLN, which increased with the rise in CS content. The highest loading capacity of DOX was 0.0242 g/g for CSLN (70:30). The strong pH-sensitive behavior of DOX was also verified by its release profile. The prepared CSLN biocomposite thus can potentially be used as an effective and viable DOX carrier. These findings suggest that lignin obtained from waste of *Terminalia catappa* leaves could be utilized to enhance chitosan characteristics, decrease agricultural waste dumping, and reduce the load of doxorubicine.

Keywords: chitosan, lignin, CSLN composite, characterization, doxorubine

Introduction

Doxorubicin (DOX) is a type of anthracycline and powerful cancer-fighting medication, comprised of a naphthacenequinone nucleus connected to an amino sugar through a glycosidic bond. DOX has a similar structure to daunorubicin, but it has a hydroxyl acetyl group at the 8-position instead of an acetyl group. DOX has limited solubility in normal saline and low solubility in alcohol, but it exhibits wide-ranging effectiveness against neoplasms, lymphomas, solid tumors, and breast tumors (Rahdar et al., 2021). Doxorubicin, a cytotoxic anthracycline antibiotic, is composed of an aminosugar daunosamine connected to the C7 of a tetracyclic aglycone, doxorubicinone, through a glycosidic bond. Doxorubicin has been extensively utilized in clinical settings for various types of cancers, effectively causing regression in acute leukemia, lymphomas, soft-tissue and osteogenic sarcomas, pediatric malignancies, and adult solid tumors, notably breast and lung carcinomas. Doxorubicin is frequently utilized in combination treatments with other cytotoxic medications like methotrexate, cisplatin, ifosfamide, vincristine, and etoposide (*Tan et al*., 2009).

Chitosan, a linear polysaccharide, has several distinct qualities, including biocompatibility, lack of toxicity, biodegradability, antimicrobial properties, and applications in cosmetology. The substantial swelling of chitosan in liquid environments causes a notable decline in its mechanical properties, alters surface structure, and ultimately hinders cell adhesion

* Second Prize (2024)

[1] Department of Chemistry, University of Yangon, Myanmar
[2] Department of Chemistry, University of Yangon, Myanmar

and growth on its surface. Many writers have recommended altering chitosan characteristics by including lignin. Besides cellulose and proteins, lignin is also a prominent natural polymer that is receiving significant interest from researchers, particularly those in the field of biomedicine (*Rosova et al*., 2021).

Lignin (LN), a phenolic polymer originating from phenylpropanoid units, represents a form of eco-friendly synthesis. This eco-friendly natural polymer, produced from industrial wood processing, is commonly used as a renewable bioresource for making various items like detergents, surfactants, and dispersants. Various techniques, such as alkylation, destruction, and sulfonation, are used to create LNs. These materials possess eco-friendly characteristics like biodegradability, biocompatibility, and low toxicity, making them useful for biomedical purposes. Their unique aromatic structure enables them to be easily absorbed at different interfaces. That is the reason why interfacial stabilization is seen as a very promising application for lignin particles, particularly when it comes to encapsulating sensitive drugs like DOX (*Rahdar et al*., 2021).

This research work focuses on the following key contributions: synthesis of chitosan−lignin biocomposite materials; characterization of chitosan−lignin bicomposite materials using SEM, FTIR, XRD, TGDTA, and UV-Vis analyses; and investigation of the doxorubicin loaded nature on chitosan−lignin biocomposite materials.

Materials and Methods

Lignin were prepared from waste of *terminalia catappa* leave. Chitosan was purchased from the British Drug House (BDH) Chemical Ltd, England. All other chemicals used were of analytical reagent grade. In all investigations, the recommended standard methods and techniques involving both conventional and modern methods were provided.

Isolation of Lignin Derived *Terminalia Catappa* Leaves

Dried fibres were treated with 4 w/v % NaOH solution at 80 °C by continuous stirring for 6 h. After the treatment, fibres were filtered and washed with distilled water until neutral pH was obtained. The resulting black liquor was filtered with Whatman filter paper to remove degraded carbohydrates and inorganic salts. Lignin separation was carried out by acidifying the black liquor to pH 2 by gradually adding 20 v/v % H_2SO_4 solutions. The suspension was then centrifuged at 7000 rpm for 15 min to separate the lignin particles, which were later collected and washed with 0.001 M H_2SO_4. Both acidification and washing steps were carried out under constant stirring. Again, the suspension was centrifuged (7000 rpm, 15 min) to separate lignin from the acidic solution. The isolated lignin was freeze-dried at − 20 °C for 24 h and ground to powder form using a motor and pestle. The stock lignin powder was stored in an airtight, dark colour glass bottle for further processing and characterization (Perera *et al*., 2023).

Synthesis of Chitosan-Lignin Biocomposite

The 3 g of chitosan (CS) powder was dissolved in 3 % v/v acetic acid solution to obtain 3 % v/v CS solution by using magnetic stirrer at room temperature for 1 h. The 3 g of lignin (LN) powder was dissolved in distilled water to obtain 3 % w/v lignin solution. The 3 % CS solution and 3 % lignin solution were mixed with the volume ratios of 70:30, 60:40, 50:50, 40:60, and 30:70 through stirring for 6 h to obtain homogeneous and viscous CSLN solutions. After that, the viscous CSLN solution was placed in freezer at – 20 °C for 48 h. The viscous CSLN was thawed

at room temperature. The CSLN composite solution was centrifuged (7000 rpm, 15 min) to separate CSLN biocomposite. The CSLN biocomposite was dried in oven at 60 °C for 8 h and ground to powder form using a motor and pestle.

Characterization of Chitosan-Lignin Biocomposite

The prepared LN and CSLN biocomposite samples were analysed by FTIR in a wide range of wavelengths between 400 cm^{-1} and 4000 cm^{-1} with a resolution of 1 cm^{-1} and 3 scans/sample. A Perkin Elmer GX System FT-IR spectrophotometer was used. A SEM study of the prepared blend films was carried out by JSM–5610 LV. Scanning Electron Microscope, JEOL at 20 kV. The dried sample powder was placed and sputter coated with platinum using a microscope sputter coater and viewed through the microscope. An X-ray powder diffractometer (XRD) was used to perform X-ray diffraction studies with Ni filtered Cu Kα X-ray radiation. UV–Vis diffuse reflectance spectra of the solids were collected from 180 to 800 nm using a UV-2550 spectrophotometer (Shimadzu) at room temperature. Thermogravimetric analysis was carried out in a nitrogen atmosphere at a heating rate of 20.0 kJ min^{-1} and scanning from 30 ^{o}C to 600 ^{o}C. Thermogravimetric analysis was carried out in a nitrogen atmosphere at a heating rate of 15 °C/min up to a temperature range of 1400 °C on the DTG-60H thermal analyzer.

Determination of Gel content

About 0.1 g of CS, LN and CSLN biocomposite was poured in phosphate buffer solution at room temperature for 2 days. Every 12 hours, the phosphate buffer solution was changed in the sample container to eliminate soluble components from the hydrogel. Subsequently, swollen samples were removed, dried at 50 °C in an oven, and weighed (Gholamali and Yadollahi, 2020). The gel content of biocomposites was calculated by the following equation.

$$\text{Gel content (\%)} = \frac{\text{Final weight of dried sample (g)}}{\text{Initial weight of dried sample (g)}} \times 100\ \%$$

Determination of Swelling Ratio

The swelling ratios of CS, LN and CSLN biocomposite were measured in phosphate buffer solutions at pH 1.2, 6.8, and 7.4 respectively, at ambient temperature. Specifically, 0.1 g of the prepared CS, LN and CSLN biocomposite was submerged in 50 mL of phosphate buffer solution (pH= 1.2, 6.8, and 7.4) at ambient temperature for 360 min to reach the swelling equilibrium. To measure the swelling ratio, the hydrogels were extracted from the phosphate buffer solution and weighed (Gholamali and Yadollahi, 2020). The swelling ratio of biocomposite was calculated by the following equation.

$$\text{Swelling ratio (\%)} = \frac{\text{Final weight (g)}}{\text{Initial weight (g)}} \times 100\ \%$$

Determination of Antimicrobial Activity

The antimicrobial activity of CS, LN and CSLN biocomposite were carried out by agar well diffusion method at Pathein University, Myanmar. Eight microorganisms namely *Escheerichia coli* (AHU5436), *Candida albicans* (NITE09542) , *Bacillus subtilis* (IFO90571), *Staphylococcus aurous* (AHU8465), *Pseudomonas fluorescens, Agrobacteriumb tumefaciens* (NITE09678), *Bacillus pumilis*(IFO12092), *and Micrococcus luteus* (NITE83297) were used for this test.

Determination of Drug Loading Study

The loading of doxorubicin (DOX) in CS, LN and CSLN biocomposite powder was carried out as follows: 0.3 g of the prepared dry biocomposite powder was swollen in 30 mL of aqueous solution containing doxorubicin (200 ppm in distilled water). After continuous stirring at 25 °C for 48 h under dark conditions, the composites were washed. Next, the absorbance of doxorubicin at 483 nm was used to calculate its loading capacity by UV-Vis spectroscopy with a specific equation (Gholamali and Yadollahi, 2020).

$$\text{Drug loading (g/g)} = \frac{\text{Weight of the drug in hydrogel (g)}}{\text{Weight of hydrogel (g)}}$$

Determination of Drug Release Study

0.1 g of CS, LN and CSLN biocomposite containing DOX was immersed under continuous stirring (50 rpm) in 10 mL of the selected release media (pH 1.2, 6.8, and 7.4) at 37 °C for 24 h. At the assigned time intervals, 5 mL of the release media was collected and the amount of drug released was determined by measuring its absorbance at 483 nm using a UV spectrophotometer. To adjust the total volume of the solution, the volume of the solution was kept constant at the same volume each time after sampling by adding fresh phosphate buffer solution. UV–Vis spectroscopy was applied to determine the amount of drug released from the CS, LN and CSLN biocomposite, with the amount of doxorubicin measured using a standard calibration curve obtained under the same conditions.

Results and Discussion

Formation of CSLN Biocomposite Nature

When the chitosan with positive charge and the lignin with negative charge were mixed together, CSLN biocomposite was formed by the electrostatic interaction between the chitosan's amino groups and the lignin's carboxyl groups. Figure 1 displays the interactions found in chitosan-lignin biocomposite. The possible cause of all the interactions between chitosan and lignin is the formation of weak hydrogen bonds. The phenolic ring of lignin contains a hydroxyl group that can bond with the glycosidic oxygen of β-1,4 (illustrated by dashed line 1 in Figure 1) and the hydroxyl group of chitosan (dashed line 3). A weak bond is also formed between the hydroxyl group of chitosan and the methoxy group of lignin (dotted line 2). Finally, a weak interaction is also observed between the aromatic ring of alkali lignin and the secondary amino group of chitosan (dotted line 4) (Nair *et al*., 2014).

In order to research the loading of doxorubicin, the hydrophobic phenylalanine unit of lignin comes together in water to create a core for micelles, while the hydrophilic hydroxyl and carboxyl units of lignin simultaneously form a shell for the micelles, allowing for the encapsulation of hydrophobic anticancer drugs like doxorubicin. Addressing the issue of low water solubility of DOX can be resolved (Chai *et al*., 2021).

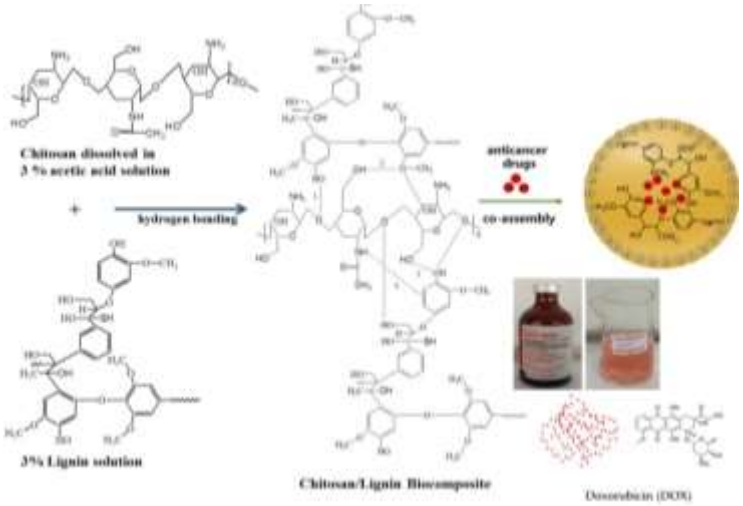

Figure 1. Preparation of chitosan–lignin biocomposite loaded with doxorubicin (Nair *et al*., 2014; Chai *et al*., 2021)

FT IR spectra analysis

The FTIR spectra of the functional groups of raw chitosan, raw lignin, and the chitosan-lignin biocomposite are presented in Figure 2. The chitosan spectrum shows the presence of -OH and -NH groups at 3352–3295 cm^{-1}. The peaks at 2927 and 2869 cm^{-1} are attributed to C–H stretching of the alkyl group. The peak at 1651 cm^{-1} represents bending of N–H in primary amine group. Small peaks at 1588 cm^{-1} are due to bending of N–H of secondary amine. A peak at 1375 cm^{-1} corresponds to C–H bending of alkyl group. The peaks at 1151 and 1061 cm^{-1} are related to C–O stretching in the β-1,4-glycosidic linkage present in chitosan. The peak at 669 cm^{-1} is due to the out-of-plane bending of the O–H group (Nair *et al*., 2014).

A broad peak at 3331 cm^{-1} corresponding to stretching of phenolic and aliphatic –OH group is observed for lignin. The peaks at 2918 and 2850 cm^{-1} are attributed to the stretching of C–H bond present in the aromatic, methoxy and alkyl groups. The peaks at 1515 cm^{-1} are typical of aromatic C=C stretching in the phenolic group of lignin (Lü *et al*., 2012). The peaks at 1446, and 1331 cm^{-1} correspond to O–H bending of the phenolic group. The peak at 1230 cm^{-1} are due to C–O–C stretching in α-O-4 and β-O-4 linkages of alkali lignin, respectively. The peaks at 1100 and 1031 cm^{-1} are due to C-O-C stretching in the alkyl substituted ether. The peak at 624 cm^{-1} is due to the S–C stretching in thioether group.

The FT-IR spectra of the CSLN biocomposite had all the key features of chitosan and lignin with minor shifts and changes in peak intensities corresponding to the weak interaction between the two components as shown in Figure 2(A). The disappearance of peak at 1588 cm^{-1} present in chitosan and the change in intensity of the peak of aromatic ring at 1531 cm^{-1} are due to the interactions between aromatic ring of alkali lignin and the secondary amine group of chitosan. There are shifts observed in the peaks corresponding to C–O stretching from 1151 cm^{-1} to 1158 cm^{-1} of β-1,4-glycosidic linkage in the chitosan, and 1061 cm^{-1} to 1054 cm^{-1} of alkyl substituted ether of the alkali lignin . All the clearly measurable changes in wave number indicate obvious interactions among the hydroxyl, carbonyl and ether groups of the two components. It can be attributed to the hydrogen bonding possibly formed between hydroxyl, carbonyl groups in chitosan and carbonyl, hydroxyl, ether groups in lignin. However, not much change of N-H stretching can be observed, which is located at 3366 cm^{-1} for both the blend and pure chitosan. The same situation can be seen for the bands of amide II.

This finding implies that the main interaction between chitosan and lignin is through hydrogen bonding involving hydroxyl and carbonyl groups, as depicted in Figure 2(B) (Chen *et*

al., 2009). These interactions refer to the hydrogen bonding between the hydroxyl group of alkali lignin and the β-1,4-glycosidic linkage of chitosan, as well as the interaction between the alkyl substituted ether of alkali lignin and the hydroxyl group of chitosan. Ibrahim *et al*. (2021) suggested that another potential interaction might be the electrostatic attraction between the chitosan amino group and the lignin carboxylic group, as shown by the peak at 1599 cm^{-1}. No notable difference was observed in the peaks of primary amine, indicating that there was no involvement of primary amine groups of chitosan in the creation of the composite.

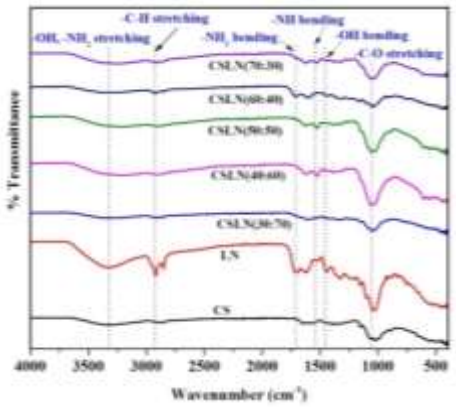

Figure 2(A). FT IR spectra of CS, LN and CSLN composites

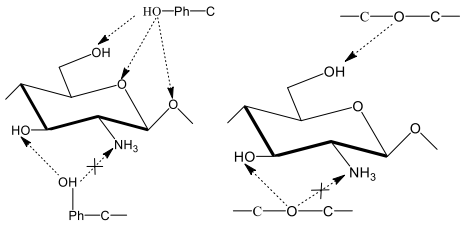

Figure 2(B). Formation of hydrogen bond formed between chitosan and lignin molecule (Chen *et al*., 2009)

X-ray diffraction analysis

The XRD spectra of chitosan and the composites containing various amounts of lignin are shown in Figure 3. It is seen that the pattern for chitosan in the base form contained three diffraction maximums at 2θ = 10.5°, 15.3°, and 20.5° (values of interplanar distances d = 8.45 Å, 5.84 Å, and 4.39 Å, respectively), which agrees with the data presented in the literature (Ogawa *et al*., 1992). The existence of peaks at 2θ = 10.5° and 15.3° confirms that both hydrated and anhydrous forms of chitosan are present in the composites. Incorporating lignin into chitosan resulted in the biocomposites becoming amorphous. Moreover, the peaks at 2θ = 10.5° were more prominent, whereas the peaks at 2θ = 15.3° were less intense for composite compared to the original chitosan. This indicates a rise in the amount of hydrated forms and a decrease in the amount of anhydrous forms when lignin is added (Rosova *et al*., 2021). The percentages crystallinity were determined as 63.06 % for CS, 31.49 % for LN, 28.42 % for CSLN (30:70), 21.62 % for CSLN (40:60), 17.71 % for CSLN (50:50), 23.07 % for CSLN (60:40), and 21.79 % for CSLN (70:30). The XRD peaks of biocomposite with lignin were stronger, suggesting that adding lignin to the chitosan matrix might lower its crystallinity. A less intense and wider peak suggested that chitosan turned into an amorphous structure after conjugation with lignin (Rai *et al*., 2017).

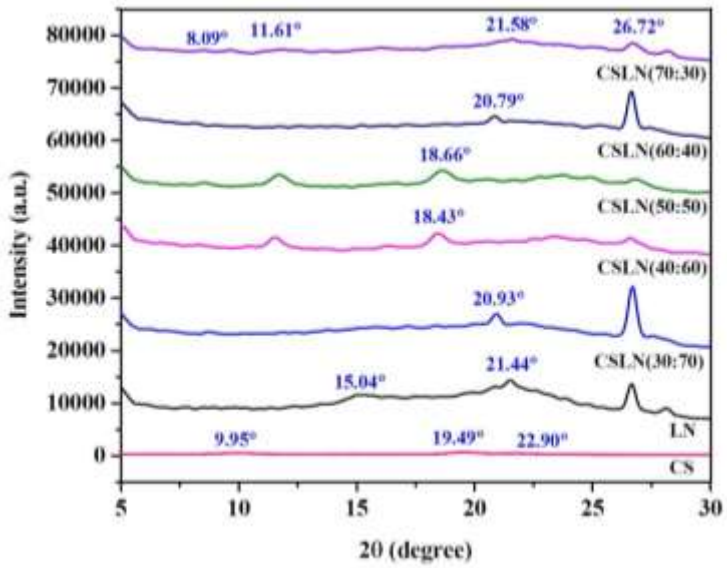

Figure 3. XRD patterns of CS, LN and CSLN composites

SEM Analysis

The morphology of CS, LN, CSLN (30:70), CSLN (40:60), CSLN(50:50), CSLN(60:40) and CSLN(70:30) were observed with SEM as shown in Figure 4. As can be seen from Figure 4(A), the surface fold of chitosan shows a tight shape of polymeric fiber and accompanied by a few holes. The results of the SEM studies demonstrated that the pure chitosan had a smooth flat surface (Figure 4A). Lignin here is composed of agglomerates containing irregular shaped particles (Figure 4B). The surface characteristics of the composites were distinct from those of the original chitosan and lignin samples (Figure 4 C-G). The images displayed indicate the composites had textured porous surfaces. As the lignin content in the samples increased, the scale and number of pores in the texture also increased.

Size distributions (Figure 4 H-L) were evaluated by measuring at least 300 particles from SEM micrographs. The results are obtained that the average diameters of the obtained biocomposites are 7.41 μm for CSLN(30:70), 19.63 μm for CSLN(40:60), 16.05 μm for CSLN(50:50), 6.77 μm for CSLN(60:40), and 6.77 μm for CSLN(80:20) respectively.

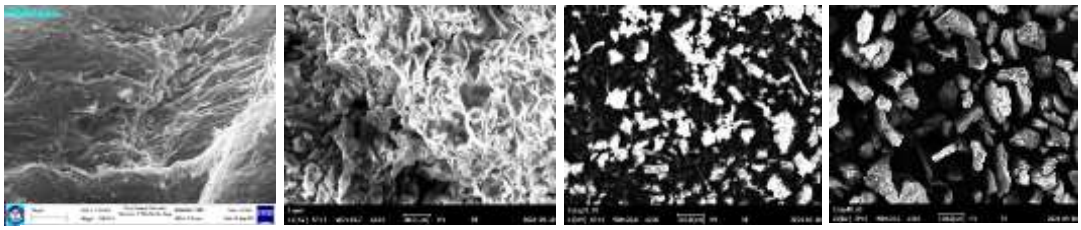

(A) CS (B) LN (C) CSLN(30:70) (D) CSLN(40:60)

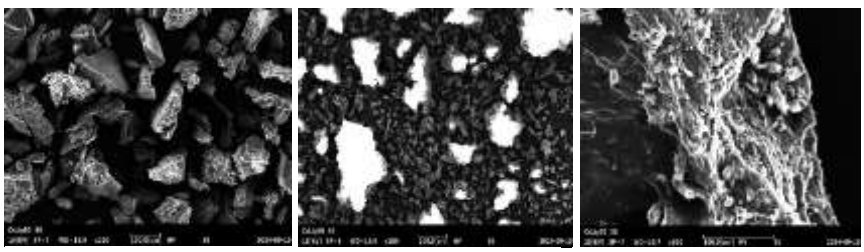

(E) CSLN(50:50) (F) CSLN(60:40) (G) CSLN(70:30)

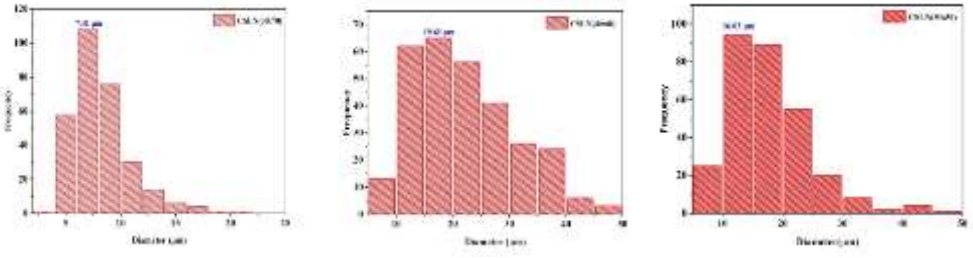

(H) CSLG(30:70) (I) CSLG(40:60) (J) CSLG(50:50)

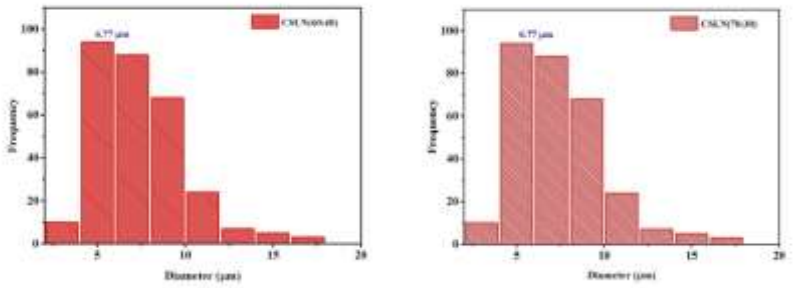

(K) CSLG (60:40) (L) CSLG(70:30)

Figure 4. SEM images of (A) CS, (B) LN, (C-G) CSLN composites and (H-L) the corresponding statistical histograms

Thermogravimetric analysis

Thermogravimetric curves, determined for CS, LN and CSLN biocomposite, are presented in Figure 5. Initial weight loss around 100 °C observed for CS, LN and CSLN can be ascribed to the removal of physisorbed moisture from the samples. Final weight losses observed for various samples at 600 °C follows the order: CS (96.25 %) > LN (95.32 %) > CSLN (60:40) (96.20 %) > CSLN (40:60) (93.47 %) > CSLN(70:30) (91.69 %) > CSLN(30:70) (87.89 %) > CSLN(50:50) (78.72 %), respectively. It is clear that lower extent of decomposition occurs as increasing lignin content that leads to the formation of a crosslinked and condensed matrix of aromatic structures at high temperatures. In order to ascertain the temperature, range of decomposition of these materials, differential weight loss profiles were plotted as depicted in Figure 5.

It is clear that chitosan exhibits a single-step, sharp decomposition in the temperature range of 210–410 °C while lignin and all CSLN biocomposite decompose in a wide temperature range of 140–600 °C. All CSLN biocomposite also exhibits a lower percent degradation in the temperature range of 220–330 °C compared to LN. Interestingly, the CSLN biocomposite decomposes in the range of 150–500 °C, with a sharp peak at 321, 324, 344, 341, and 317 °C respectively. This temperature corresponds to the maximum weight loss rate, as observed in the differential weight loss profile. A similar peak was also observed for chitosan at 307 °C. However, there is no sharp transition for lignin and CSLN biocomposite. This demonstrates that within the physical blend, the breakdown of each component has an accumulative impact due to the distinct phases of chitosan and lignin. Nevertheless, the CSLN biocomposite is homogeneous in terms of binding of chitosan and lignin via weak hydrogen bonds, and hence decomposes gradually without any signature peak of chitosan (Nair *et al*., 2014).

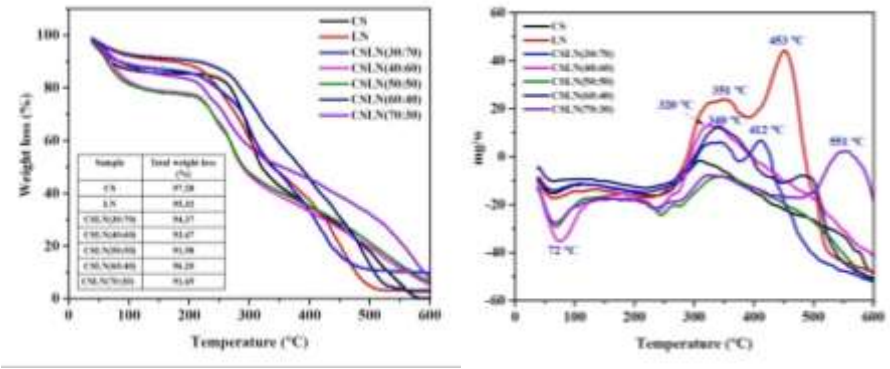

Figure 5. (A) TG curves and (B) DTA curves for CS, LN and CSLN biocomposites

UV-vis absorption spectra

The UV-visible spectral (200-500 nm) of pure CS, LN and CSLN biocomposite particles were used to confirmation for the any modifications conjugation occurred between them. The individual's component and CSLN biocomposite UV-visible spectra are shown in Figure 6. As seen in Figure 6, The CS peaks showed an absorption peak at 294 nm whereas LN peaks shows two characteristics absorption peaks at 256 and 365 nm. As a structural unit of lignin, the aromatic compound group (CO) and alkene bonds (C=C) giving lignin its two characteristics absorption peaks or the UV spectrum at 200-230 nm and 260-280 nm (Lee *et al*., 2013).

Various peaks have been appeared in CSLN biocomposite particles such as 255 and 357 nm for CSLN (30:70), 255 and 360 nm for CSLN (40:60), 255 and 360 nm for CSLN (50:50), 257 and 361 nm for CSLN(60:40), and 254 and 358 nm for CSLN(70:30), which could be attributed to the lignin present in the chitosan. The second another special properties have proved the conjugation occurred between them due to the shifting of absorption spectra from blue region to red region has been in CSLN biocomposite particles (Rai *et al*., 2017).

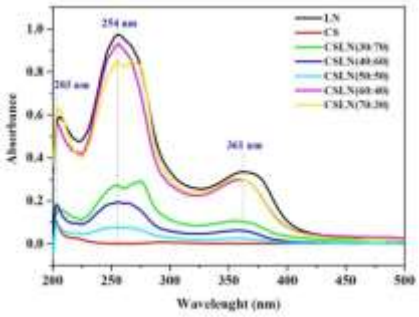

Figure 6 UV-Visible spectra curves of CS, LN and CSLN composites

Gel content

The gel content is a measure of how the polymer chains are linked together in the composite structure. The level of crystallinity and the extent of cross-linking are determined by how the components of the composite interact with each other. Figure 7 shows the fluctuating gel content, ranging from 42 % to 96 %. The gel content rose as the CS ratio in the hydrogel structure went up and dropped as the ratio increased. Nevertheless, when the CS amount rose to 30 % and 70 %, there was an increase in gel content (Gholamali *et al.*, 2019).

Swelling Behaviour

The swelling behavior of the LN, CS and CSLN biocomposite particles was assessed at 25 °C in the pH of 1.2, 6.8 and 7.4 in order to study the pH sensitivity of the prepared biocomposites. As shown in Figure 8, the weight at different time points was monitored to explain the water absorption process of the CS, LN, and CSLN biocomposite. All of the biocomposite reached the swelling equilibrium with the maximum value at 6 h in this investigation periods. At 6 h, the swelling ratios was found CS, LN, CSLN biocomposites were 65 % for LN, 82 % for CS, 97 % for CSLN(30:70), 105 % CSLN(40:60), 113 % CSLN(50:50), 127 % CSLN(60:40), and 137 % CSLN(70:30) at pH 1.2; 76 % for LN, 85 % for CS, 114 % for CSLN(30:70), 129 % CSLN(40:60), 118 % CSLN(50:50), 147 % CSLN(60:40), and 176 % CSLN(70:30) at pH 6.8, and 80 % for LN, 104 % for CS, 129 % for CSLN(30:70), 132 % CSLN(40:60), 159 % CSLN(50:50), 177 % CSLN(60:40), and 188 % CSLN(70:30) at pH 7.4 respectively. It was observed that the swelling degree of prepared biocomposite at pH 7.4 and 6.8 was higher than that of pH 1.2, as in the higher pH (6.8 and 7.4), sulfonate groups in the chemical structure of lignin formed ionic bonds with amino groups in the chemical structures of chitosan leading to higher electrostatic repulsion and thus, water penetrating into the hydrogel matrix.

The swelling ratio of the CSLN was observed to rise as the CS content increased. The amount of water absorbed was mainly impacted by the content of CS. CSLN biocomposite exhibited greater swelling ratio than LN and CS, due to the combined effect of hydrophilic groups and porous structure in increasing swelling capacity (Zhang *et al*., 2019)

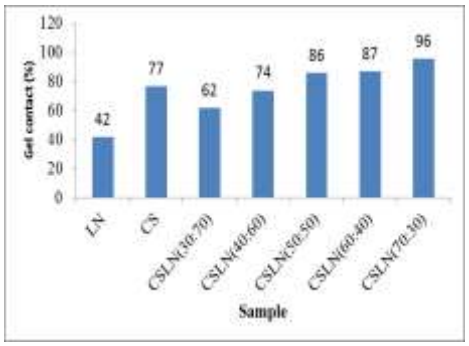

Figure 7. Gel content of CSLN biocomposite in different samples

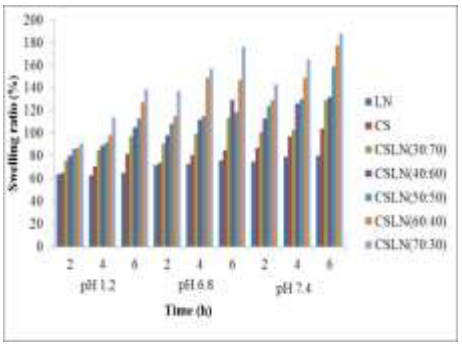

Figure 8. Swelling behavior of CSLN biocomposite at pH values of 1.2, 6.8 and 7.4 in different samples

3.7 Antimicrobial of CSLN Biocompos

The antimicrobial effect of the CSLN biocomposites have been tested against *Bacillus subtilis, Staphylococcus aureus, Pseudomonas fluorescens, Bacillus pumilus, Candida albicans, Escherichia coli, Agrobacterium tumefaciens,* and *Micrococcus luteus* and their inhibitory zone results are given in Figure 9 and Table1. The potential antimicrobial activity of all CSLN biocomposites is evident from the Figure 9 and Table1. Gram-positive bacteria are typically more susceptible to aromatic compounds or antibiotics in comparison to gram-negative bacteria. The discrepancy in the outer membrane composition of gram-positive and gram-negative bacteria may offer a reason for this observation. Gram-positive bacterial cell walls contain a higher amount of lipoproteins and phospholipids compared to gram-negative bacteria, potentially increasing the permeability of hydrophobic compounds (Rai *et al*., 2017). Based on their antimicrobial effectiveness, it is determined that the CSLN biocomposites could be used as antibiotic agents.

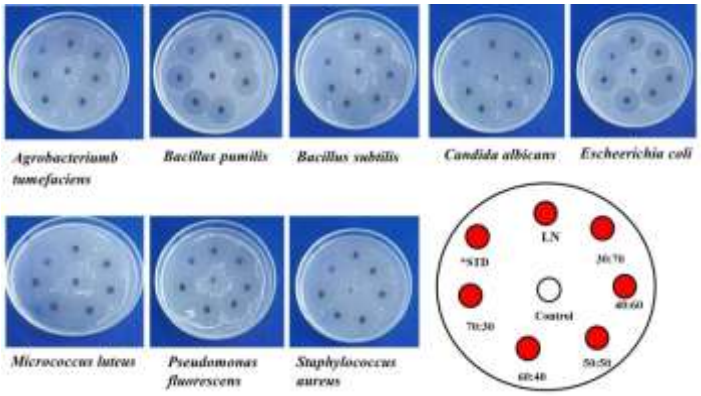

Figure 9. Antimicrobial properties of CSLN biocomposite

Table 1. Inhibition Zone Diameters of CSLN Biocomposites

Microorganisms	Inhibition zone diameters (mm)						
	LN	CSLN (30:70)	CSLN (40:60)	CSLN (50:50)	CSLN (60:40)	CSLN (70:30)	*STD
A. tumefaciens	24.0	25.1	26.5	26.8	26.9	27.1	27.5
B. pumilis	23.9	26.2	26.3	26.4	26.7	26.9	26.3
B. subtilis	24.5	24.6	24.8	25.1	26.7	26.8	27.2
C. albicans	27.5	27.7	27.9	28.2	28.3	28.6	27.6
E. coli	24.8	24.9	25.5	25.6	25.7	25.9	27.1
M. luteus	26.0	26.1	26.4	26.8	27.3	27.5	26.5
P. fluorescens	27.0	27.2	27.5	27.8	28.0	28.5	27.6
S. aureus	27.1	27.3	27.6	27.9	28.2	28.6	27.5

For Bacterial *STD = Chloramphenicol, For Fungus *STD = Nystatin

Agar well diameter - 8 mm, 10 mm - 14 mm = low activity
15 mm - 19 mm = good activity, 20 mm and above = very high activity

Drug Loading

The effect of CS, LN, and CSLN biocomposites on DOX encapsulation was investigated via the prepared biocomposite with the doxorubicin loading data obtained were described in Figure 10. The maximum loading capacity of DOX on CSLN (70:30) was 0.0242 g/g. From this figure, it is evident that the concentration of doxorubicin, an anticancer drug, loaded in the biocomposites increased as the sample amount was increased. Because of the presence of hydrogen bonding and electrostatic attraction interactions between DOX and CSLN biocomposites. These interactions led to a higher drug loading percentage in the biocomposite with a high concentration of CS.

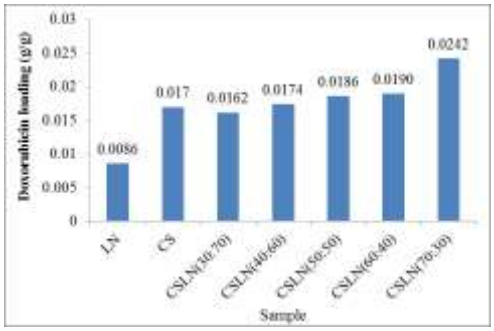

Figure 10. The amount of doxorubicin loaded into CS, LN, and different CSLN samples

Drug Releasing

The behavior of drug release of DOX loaded CSLN biocomposite at various pH of 1.2, 6.8 and 7.4 were studied for 300 min. Also, the relationship between release of doxorubicin composite versus time was examined with the volume ratios of CS and LN as shown in Figures 11(A), (B), and (C). As seen in figures 11(A), (B), and (C), the highest amount of drug release in composite at 300 min in phosphate buffers at pH 6.8 and 7.4 was compared to pH 1.2. The drug release of doxorubicin from DOX loaded onto neat CS, LN and CSLN biocomposites in pH 1.2, ~~and~~ ~~pH~~ 6.8 and 7.4, phosphate buffers revealed different release mechanisms which depended on the type of cationic ions in the release medium. A possible explanation for this may be that in pH 1.2, hydrogen bonds in CSLN caused creation of hydrophobic networks a collapsed state. These factors can lead to the formation of insoluble CSLN for reserved drug release; hence, doxorubicin release from the hydrogels can be described by a controlled matrix diffusion mechanism. Nevertheless, at pH 6.8 and 7.4 of phosphate buffer, the carboxylic acid groups in the LN became ionized on the CS chains causing elevated osmotic pressure and increased electrostatic repulsion between charged groups. Thus, the maximum swelling was observed at pH 7.4 phosphate buffer for CSLN biocomposites. As indicated in Figure 11(A), (B), and (C), the release rate of DOX loaded on the biocomposites increases with decreases in the amount of LN, which plays a key role in prolonging drug release time of the LN in the nanocomposite. In addition, electrostatic adsorption interactions and the hydrogen bonding between LN in biocomposite and doxorubicin could reduce the initial release of DOX from the prepared biocomposite (Gholamali, 2019; Zare-Akbari *et al*., 2019).

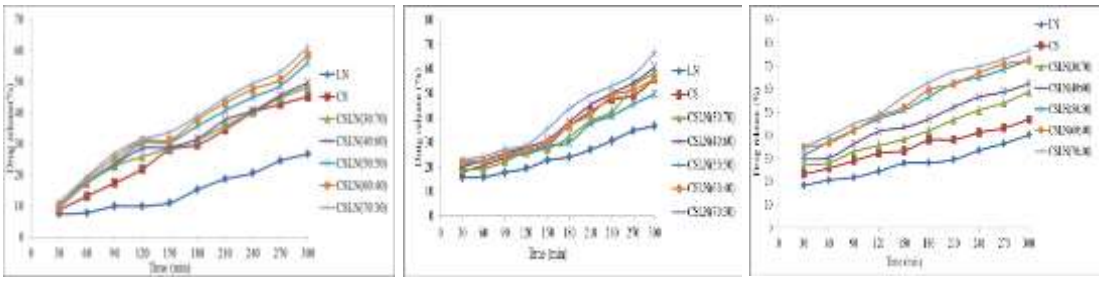

(A) pH 1.2 (B) pH 6.8 (C) pH 7.4

Figure 11. The percentage of drug released from CS, LN and CSLN biocomposites at pH values of (A) 1.2 (B) 6.8 (C) 7.4

Conclusion

In the present work, the biocomposite chitosan-lignin was successfully synthesized with different compositions of chitosan and lignin which were used for the delivery of anticancer drugs. *Terminalia catappa* leaf was used as a raw material to produce lignin (LN). The structural details of the CSLN biocomposite were characterized by FT-IR, XRD, SEM, TG-DTA, and UV-Vis techniques. FTIR absorption peaks corresponded to the chitosan hydroxyl, carbonyl and ether groups in lower wave number, indicating some weak interaction occurred such as hydrogen-bonding in between CS and LN. XRD peaks of LN containing CSLN biocomposites were more intense, indicating that the interaction of LN into the composite matrix which induces an increase in crystallinity nature. SEM images showed good dispersion as the content of lignin. The surface of lignin-containing biocomposites was porous and textured. With an increasing lignin content in the composite, the amount of pores increased, and the surface texture became more pronounced. TG-DTA data suggest that in addition to increasing the thermal stability of the samples and the residual content, the thermal degradation in the samples containing LN is greater than in the samples without the LN. The UV-vis spectra showed that conjugation occurred between CS and LN. The swelling behavior of biocomposite was studied at pH 1.2, 6.8 and 7.4. The results indicated that the swelling ratio of CSLN biocomposite was significantly enhanced compared to pure CS and LN, which depended on the concentration of CS and LN. All CSLN biocomposites show potential antimicrobial activity. Doxorubicin was selected as an anticancer drug with the loading and release capacity of the drug in different biocomposite calculated. The loading and release behavior of doxorubicin in CSLN showed that CSLN loaded the drug better than pure did, but the drug release from neat CS and LN was higher than that of biocomposite. Based on these findings, it can be concluded that the prepared CSLN biocomposite prolonged the cumulative DOX release into phosphate buffer solution at pH 1.2, 6.8 and 7.4. Therefore, the CSLN biocomposite can be introduced as a new bio-compatible carrier for controlled delivery of anticancer drugs such as doxorubicin with pH-responsive properties.

The contribution of the present work is the synthesis of chitosan-lignin biocomposite and may be used for anticancer drugs.

Acknowledgements

The author feel indebted to Professor and Head Dr. Ni Ni Than, Department of Chemistry, University of Yangon, Myanmar, for her suggestions.

References

Aung Than Htwe, Hnin Wutt Yee Htun, Yamin Thet, May Thazin Kyaw, Ngwe Sin, Win Pa Pa Phyo and Cho Cho. (2023). "Doxorubicin-Loaded Carboxymethyl Cellulose/Chitosan/ZnO Nanocomposite Hydrogel Beads as an Anticancer Drug Carrier Agent", *JARC-UY.*, 9(1&2), 1-17

Chai, Y., Y. Wang, B. Li, W. Qi, R. Su and Z. He. (2021). "Microfluidic Synthesis of Lignin/Chitosan Nanoparticles for the pH-Responsive Delivery of Anticancer Drugs". *Langmuir*, vol. 37, pp. 7219-7226

Chen, K., Y. Qian, C. Wang, D. Yang, X. Qiu and B. P. Binks. (2021). "Tumor Microenvironment-Responsive, High Internal Phase Pickering Emulsions Stabilized by Lignin/Chitosan Oligosaccharide Particles for Synergistic Cancer Therapy". *Journal of Colloid and Interface Science*, vol. 591, pp. 352-362

Chen, L., C. Tang, N. Ning, C. Wang, Q. Fu and Q. Zhang. (2009). "Preparation and Properties of Chitosan/Lignin Composite Films". *Chinese J. Polym. Sci.*, vol. 27, pp. 739-746

Gholamali, I., M. Asnaashariisfahani and E. Alipour. (2019). "Silver Nanoparticles Incorporated in pH-Sensitive Nanocomposite Hydrogels Based on Carboxymethyl Chitosan- Polyvinyl Alcohol for Use in a Drug Delivery System", *Regen. Eng. Transl. Med.*, pp. 1-16

Gholamali, I. and M. Yadollahi. (2020). "Doxorubicin-Loaded Carboxymethyl Cellulose/Starch/ZnO Nanocomposite Hydrogel Beads as an Anticancer Drug Carrier Agent". International Journal of Biological Macromolecules, vol. 160, pp. 724-735

Ibrahim, S., N. S. S. Kanal, M. A. M. Hanafiah, N. F. Ariff and S. H. Saleh. (2021). "Chitosan-Lignin Composite for Recovery of Lanthanum(III) Ions from Aqueous Solutions". Malaysian Journal of Analytical Science, vol. 25(5), pp. 848-857

Lee, R. A., C. Bedard, V. Berberi, R. Beauchet, and J. M. Lavoie. (2013). "UV-vis as Quantification Tool for Solubilized Lignin Following a Single-Shot Steam Process", *Bioresource Technology,* vol. 144, pp. 658-663

Lü, Q. F., Z. Huang, B. Liu, and X. Cheng. (2012). "Preparation and Heavy Metal Ions Biosorption of Graft Copolymers from Enzymatic Hydrolysis Lignin and Amino Acids". *Bioresour. Technol.*, vol. 104, pp. 111-118

Nair, V., A. Panigrahy and Vinu. (2014). "Development of Novel Chitosan-Lignin Composites for Adsorption of Dyes and Metal Ions from Wastewater", *Chemical Engineering Journal*, vol. 254, pp. 491-502

Ogawa, K., T. Yui and M. Miya. (1992). "Dependence on the Preparation Procedure of the Polymorphism and Crystallinity of Chitosan Membranes", *Biosci. Biotechnol. Biochem*., vol. 56, pp. 858–862

Perera, U.P., M.L. Foo and I.M.L. Chew. (2023). "Synthesis and Characterization of Lignin Nanoparticles Isolated from Oil Palm Empty Fruit Bunch and Application in Biocomposites". *Sustainable Chemistry for Climate Action*, vol. 2, pp. 1-12

Rai, S., P.K. Dutta and G.K. Mehrotra. (2017). "Lignin Incorporated Antimicrobial Chitosan Film for Food Packaging Application". *J. Polym. Mater.*, vol. 34(1), pp. 171-183

Rahdar, A., S. Sargazi, M. Barani, S. Shahraki, F. Sabir and M.A. Aboudzadeh. (2021). "Lignin-Stabilized Doxorubicin Microemulsions: Synthesis, Physical Characterization, and In Vitro Assessments". *Polymers*, vol. 13(641), pp. 1-14

Rosova, E., N. Smirnova, E. Dresvyanina, V. Smirnova, E. Vlasova, E. Ivankova, M. Sokolova, T. Maslennikova, K. Malafeev, K. Kolbe, M. Kanerva and V. Yudin. (2021). "Biocomposite Materials Based on Chitosan and Lignin: Preparation and Characterization". *Cosmetics*, vol. 8(24), pp. 1-17

Tan, M.L., P.F.M. Choong and C.R. Dass. (2009). "Review: Doxorubicin Delivery Systems Based on Chitosan for Cancer Therapy". *Journal of Pharmacy and Pharmacology*, vol. 61, pp. 131-142

Urion, K., P. R. Bodart, P. Winckler, J. Raya, R. D. Gougeon, P. Cayot, S. Domenek, F. Debeaufort and T. Karbowiak. (2016). "Biobased Composite Films from Chitosan and Lignin: Antioxidant Activity Related to Structure and Moisture". *ACS Sustainable Chem. Eng.*, vol. 4, pp. 6371-6381

Zare-Akbari, Z., H. Farhadnejad, B. Furughi- Nia, S. Abedin, M. Yadollahi and M. Khorsand-Ghayeni. (2019). "pH-Sensitive Bionanocomposite Hydrogel BeadsBased on Carboxymethyl Cellulose/ZnO Nanoparticle as Drug Carrier", *Int. J. Biol. Macromol.*, vol. 93, pp. 1317-1327

Zhang, Y., M, Jiang, Y. Zhang, Q. Cao, X. Wang, Y. Han, G. Sun, Y. Li, J. Zhou. (2019). "Novel Lignin–Chitosan–PVA Composite Hydrogel for Wound Dressing", *Materials Science & Engineering C*, vol. 104, pp. 1-8